Hitting the right spot: mechanism of action of OPB-31121, a novel and potent inhibitor of the Signal Transducer and Activator of Transcription 3 (STAT3)

Lara Brambilla[a,§], Davide Genini [a,§], Erik Laurini[b,§], Jessica Merulla[a], Laurent Perez[c], Maurizio Fermeglia[b], Giuseppina M. Carbone[a,d], Sabrina Pricl[b,*], Carlo V. Catapano[a,d,*]

[a]Institute of Oncology Research (IOR), Via Vela 6, 6500 Bellinzona, Switzerland

[b]Molecular Simulation Laboratory (MOSE), University of Trieste, Piazzale Europa 1, 34127 Trieste, Italy

[c]Institute of Research in Biomedicine (IRB), Via Vela 6, 6500 Bellinzona, Switzerland

[d]Oncology Institute of Southern Switzerland (IOSI), Via Vela 6, 6500 Bellinzona, Switzerland

[§]These authors contributed equally to this work

[*]Corresponding authors: sabrina.pricl@di3.units.it; carlo.catapano@ior.iosi.ch

STAT3 is a key element in many oncogenic pathways and, like other transcription factors, is an attractive target for development of novel anticancer drugs. However, interfering with STAT3 functions has been a difficult task and very few small molecule inhibitors have made their way to the clinic. Recently, OPB-31121, a compound currently in clinical trials, has been reported to affect STAT3 signaling although its mechanism of action has not been unequivocally demonstrated. In this study we used computational experimental approaches to define the molecular target and the mode of interaction of OPB-31121 with STAT3. To validate our approach, similar studies were performed with known STAT3 inhibitors (STAT3i). Docking and molecular dynamics simulation (MDS) showed that OPB-31121 interacted with a distinct pocket in the SH2 domain of STAT3. Interestingly, there was no overlap with the sites of binding of other known STAT3i. Computational predictions were confirmed by *in vitro* binding assays, competition experiments and site-directed mutagenesis of critical residues in the OPB-31121 binding pocket. Binding assays demonstrated the remarkably high affinity of OPB-31121 for STAT3 with K_d (10 nM) 2-3 orders lower than other STAT3i. Notably, a similar ranking of the compounds was observed in terms of inhibition of STAT3 phosphorylation, cell viability and clonogenicity. These results indicate that the high affinity and efficacy of OPB-31121 might be related to its unique features and mode of interaction with STAT3. These unique characteristics make OPB-31121 an promising candidate for further clinical development and an interesting lead for designing new STAT3i.

Keywords: STAT3; transcription factors; small molecule inhibitors; anticancer drugs; cancer therapy; molecular modeling; inhibition mechanism; functional study

1. INTRODUCTION

Signal Transducers and Activators of Transcription (STATs) are a family of latent cytoplasmic proteins that once activated regulate many aspects of cell growth, survival and differentiation (Levy and Darnell, 2002; Yu et al., 2009). STAT proteins act as signal transducers and transcription factors with the ability to transmit signals from the cell membrane to the nucleus without the involvement of second messengers (Levy and Darnell, 2002; Yu et al., 2009). The STAT family includes seven members (STAT1, 2, 3, 4, 5a, 5b, and 6) that share extensive structural homology (Yu et al., 2009). The main structural motifs of STAT proteins are the N-terminal domain (NTD), coiled-coil domain (CCD), DNA-binding domain (DBD), Src Homology 2 domain (SH2) and C-terminal domain (CTD). The NTD and CCD are required for nuclear translocation and protein-protein interaction, respectively (Levy and Darnell, 2002; Lim and Cao, 2006). The DBD is necessary for the recognition of specific DNA sequence elements and binding to gene promoters. The SH2 domain is the most conserved domain of the family and is required for formation of STAT3 dimers (Lim and Cao, 2006). Phosphorylation of a specific tyrosine residue in the CTD of STAT proteins allows the interaction of the SH2 domains of monomers and formation of active dimers (Lim and Cao, 2006; Zhong et al., 1994). In the case of STAT3, phosphorylation of tyrosine 705 (pY705) is the key event to promote dimerization. Binding of cytokines and growth factors to the respective receptors and consequent activation of the receptor-associated tyrosine kinases, like Janus Kinases (JAK), induce pY705 (Yu et al., 2009). This event is critical to promote dimerization and nuclear translocation of STAT3 and activation of STAT3 transcriptional functions (Yu et al., 2009). Non-receptor-associated kinases, such as Src, also catalyze Y705 phosphorylation and activate STAT3 signaling. In addition to Y705, STAT3 is phosphorylated at serine 727 (pS727) by serine protein kinases (Zhang et al., 1995). pS727 has been described to enhance the transcriptional activity of STAT3 (Wen et al., 1995). However,

recently pS727 has been reported to control mitochondrial localization of STAT3 and mitochondrial functions (Gough et al., 2009; Wegrzyn et al., 2009). Other post-translational modifications, like acetylation and methylation, are relevant for STAT3 functions in normal and pathological conditions (Kim et al., 2013a; Lee et al., 2012; Yuan et al., 2005).

Alterations in the STAT3 signaling pathway are associated with different human diseases (O'Shea and Plenge, 2012). STAT3 is over-expressed and activated in many human cancers and promotes cell proliferation, survival, tumor angiogenesis and immune-evasion (Sansone and Bromberg, 2012; Yu et al., 2009). Activation of the JAK/STAT3 signaling pathway has been shown to contribute to tumor initiation and progression in various cancer models (Yu et al., 2014; Yu et al., 2009). Recently, activation of STAT3 has been associated with promotion and maintenance of cancer stem-like cell (CSC) properties, tumorigenicity and metastatic capability in many human cancers, including prostate cancer (Kroon et al., 2013; Marotta et al., 2011; Schroeder et al., 2014; Yu et al., 2014). Consistently, in many cancers activation of STAT3 is associated with advanced, metastatic disease and clinical progression (Sansone and Bromberg, 2012; Yu et al., 2009). The JAK/STAT3 pathway contributes also to reduced response to treatment promoting survival and development of resistance after treatment with various kinase inhibitors or androgen deprivation therapy (Lee et al., 2014; Schroeder et al., 2014; Sos et al., 2014). We have shown recently that activation of the JAK/STAT3 pathway contributes the establishment of immune-tolerance and chemoresistance in a prostate cancer mouse model through the secretion of immunosuppressive cytokines in the tumor microenvironment (Toso et al., 2014).

Over-activity of STAT3 in human cancers is frequently the result of deregulation of upstream pathways leading to activation of cytokine and growth factor receptor associated tyrosine kinases, like JAK family kinases (Grivennikov and Karin, 2008; Sansone and Bromberg, 2012; Yu et al., 2014). However, alternative pathways of STAT3 activation exist (Yu et al., 2014).

Unphosphorylated and S727 phosphorylated STAT3 control transcriptional and non-transcriptional functions of STAT3 (Meier and Larner, 2014; Timofeeva et al., 2012). Interestingly, in prostate cancer STAT3 has been reported to induce cell transformation and tumor development in the absence of pY705 (Qin et al., 2008). The oncogenic effect of STAT3 in this system depended on pS727 and transcriptional dependent and independent functions of STAT3 (Qin et al., 2008). Acetylation and methylation are also crucial for the role of STAT3 in the acquisition of cancer stem cell-like phenotype and tumorigenic progression (Kim et al., 2013a; Su et al., 2011).

Because of its central role in multiple oncogenic pathways, STAT3 is an attractive target for development of anticancer drugs and great effort has been devoted over the last decade to the discovery of selective inhibitors (Debnath et al., 2012; Yu et al., 2009). Inhibitors of STAT3 are classified as direct and indirect inhibitors (Benekli et al., 2009; Debnath et al., 2012). Indirect inhibitors are those that interfere with cytokine and growth factor receptors or the associated kinases that activate STAT3 by phosphorylation. Conversely, direct inhibitors interact with the STAT3 protein. Direct STAT3i are expected to block multiple STAT3 functions, like dimerization, nuclear translocation and DNA binding (Debnath et al., 2012). Direct inhibitors can be further divided according to their target domain, e.g. the NTD, DBD or SH2 domain. Due to its critical involvement in STAT3 activation, the SH2 domain is the most attractive target for STAT3i (Debnath et al., 2012). Indeed, SH2-targeting compounds constitute the largest class of direct STAT3i.

Many studies have demonstrated that genetic knockout, knockdown and small molecule inhibitors of STAT3 prevent tumor development and growth in preclinical models (Chan et al., 2004; Kortylewski et al., 2005). However, despite the preclinical evidence that STAT3 would be an ideal target for cancer therapy, effective strategies to inhibit STAT3 in the clinic are still lacking. This is

largely due to the intrinsic difficulty of targeting directly a transcription factor like STAT3 and the diversity of the upstream activating pathways. Consequently, few direct STAT3i have shown relevant activity in preclinical models *in vivo* and have been tested in clinical trials (Debnath et al., 2012). OPB-31121 has been recently reported to interfere with STAT3 signaling, although the underlying mechanism has not been clarified yet (Hayakawa et al., 2013; Kim et al., 2013b). OPB-31121 exhibits potent anticancer activity *in vitro* and in tumor xenografts (Hayakawa et al., 2013; Kim et al., 2013b) and is currently investigated in a number of clinical trials (https://clinicaltrials.gov). Understanding how OPB-31121 interacts with STAT3 and the basis of its potent anticancer effect would be highly relevant for further development of this and other STAT3i. In this study, we combined *in silico* and *in vitro* experiments to investigate how OPB-31121 and other small molecule inhibitors interact with STAT3 and the functional consequences of these drug-target interactions. Importantly, our study reveals a unique mode of interaction of OPB-31121 with the STAT3 SH2 domain not shared by any of the other STAT3i tested. These unique features might be at the basis of the compound efficacy and make OPB-31121 an interesting lead for further clinical development and design of new direct STAT3i.

2. MATERIALS AND METHODS

2.1. Computational studies

The crystal structures of STAT3 protein was obtained from the available pdb file 1BG1in the Protein Data Bank repository (Becker et al., 1998). All compounds structures were designed and optimized using Discovery Studio (DS, v. 2.5, Accelrys Inc., San Diego, CA, USA) (Laurini et al., 2011). All docking experiments were performed with Autodock 4.3 (Morris et al., 2009), with Autodock Tools 1.4.6 on a win64 platform following a consolidated procedure (Giliberti et al., 2010). The binding free energy, ΔG_{bind}, between each drug and the protein was estimated resorting

to the MM/PBSA (Molecular Mechanics/Poisson-Boltzmann Surface Area) approach. According to this well-validated methodology (Laurini et al., 2012), the binding free energy was obtained as the sum of the interaction energy between the receptor and the ligand (ΔE_{MM}), the solvation free energy (ΔG_{sol}), and the conformational entropy contribution ($-T\Delta S$), averaged over a series of snapshots from the corresponding MDS trajectories. The free energy of binding ΔG_{bind} and the concentration of ligand that inhibits the protein activity by 50% (i.e., IC_{50}) are related by the following fundamental equation: $\Delta G_{bind} = -RT \ln 1/IC_{50}$, where R is the gas constant and T is the temperature. Thus, once ΔG_{bind} for a given protein/inhibitor couple is estimated by MM-PBSA simulations, the relative IC_{50} value is also known by virtue of this relationship. The role of the key residues identified by PRBFED was further studied by performing computational alanine scanning (CAS) experiments (Guo et al., 2012). Accordingly, the absolute binding free energy of each mutant protein, in which one of the key residue was replaced with alanine, was calculated with the MM/PBSA method and corresponded to the difference in the binding free energy between the wild-type (wt) and its alanine mutant (mut) counterpart.

2.2. Cell lines, plasmids, chemicals and antibodies

Human prostate cancer DU-145 and LNCaP cell lines were purchased from American Type Culture Collection and maintained in RPMI supplemented with 10% (FBS) (PAA, Brunschwig, Basel, CH). STAT3 SH2 domain (amino acid residues 586-685) was subcloned into pGEX-2T vector (GE Healthcare Europe GmbH) from pET28a-STAT3-SH2 domain (GenScript USA Inc) using BamHI and EcoRI restriction sites. Mutant constructs were generated using GENEART® Site-Directed Mutagenesis System (Life Technologies). OPB-31121 (Otsuka Pharmaceutical, Tokyo, Japan), STA-21, and Stattic (ENZO LIFE SCIENCES AG, Lausen, CH), S31.201 and Cryptotanshinone (Merck KGaA, VWR, Dietikon, CH) were dissolved in DMSO. IL-6 (10 ng/ml,

R&D Systems Europe Ltd., Abingdon, UK), ampicillin (50 μg/ml, Eurobio) and IPTG (isopropyl-β-D-thiogalactopyranoside, 1 mM, Promega, Dübendorf, CH) were dissolved in sterile water. Antibodies against STAT3, pSTAT3 Tyr705, pSTAT3 Ser727, were purchased from Cell Signaling Technology (BIOCONCEPT, Allschwil, CH), and GAPDH from Millipore (Zug, CH).

2.3. Western blotting

Cells were washed once in PBS and lysed in lysis buffer (25 mM Tris-HCl pH=7.4, 50 mM KCl, 5 mM EDTA, 1% NP-40, 0.5% Sodium deoxycholate, 0.1% SDS) supplemented with protease and phophatase inhibitors cocktail (Roche Diagnostics (Schweiz) AG, Rotkreuz, CH), sodium orthovanadate (Na_3VO_4, Acros Organics) and phenylmethanesulfonylfluoride (PMSF, Sigma-Aldrich). After 20 min of incubation on ice samples were centrifuged for 15 min at 4°C and proteins were quantified using BCA Protein Assay Kit (Pierce, Perbio Science Switzerland SA, Lausanne, CH). Proteins were loaded 10-12% Sprint Next Gel (Amresco, Bioconcept, Allschwil CH) and analyzed by immunoblotting. Membranes were blocked for 1 h with 0.2% of I-Block (Life Technologies) and then probed overnight at 4°C with primary antibodies and for 1 h with horseradish peroxidase (HRP)-conjugated secondary antibodies. Western Bright ECL detection system (WITEC AG, Littau, CH) was used for detection.

2.4. Cell viability

DU145 and LNCaP cells were plated in 96-well plates in phenol red-free RPMI supplemented with 10% serum. After 24 h cells were treated with the indicated STAT3 inhibitors. Cell viability was determined using MTT assay after 72 h (Genini et al., 2012). All assays were performed in triplicate and repeated in at least three independent experiments.

2.5. Colony forming assay

Cells were plated in triplicate in 6-well plates. Drugs were added to the medium at increasing concentrations. After 10 days cells were fixed and stained with 1% crystal violet in 20% ethanol. Colonies were counted with an automated colony counter Alphaimager 3400 (Napoli et al., 2009). Results are represented as mean ± SD from 3 independent experiments.

2.6. Expression and purification of GST-STAT3 SH2 domain

Escherichia coli strain BL21(DE3) (Life Technologies) transformed with the pGEX-2T-GST-STAT3_SH2 domain plasmids (WT, S636A, and V637A mutants) or pGEX-2T-GST (100 ng of DNA) was grown at 37°C in LB medium containingampicillin (50 μg/ml) to an OD 600 of 0.6–0.7. Cells were then induced with 1 mM IPTG for 4 h at 37°C and subsequently harvested by centrifugation at 4000xg. The bacterial pellet was resuspended in cold PBS containing protease inhibitors plus 1 mg/ml of lysozyme (Sigma-Aldrich) and sonicated (30 seconds of pulsing/30 seconds of pause for 6 times). Triton X-100 (Sigma-Aldrich) was then added at afinal concentration of 1% and the lysate was centrifuged for 20 minutes at 4°C. Supernatant was filtered (0.45 μm), diluted 1:1 with cold PBS and purified by affinity chromatography using GSTrap HP column (GE Healthcare). Fusion proteins were eluted with 10 mM of glutathione, reduced, desalted in PBS and concentrated to 1 mg/ml.

2.7. Isothermal titration calorimetry

Isothermal titration calorimetry (ITC) experiments of STAT3i binding to the STAT3 SH2 domain were conducted with a Nano ITC Technology (TA Instruments) at 25°C. After temperature equilibration, GST-SH2 wt, GST-SH2S636A or GS-SH2V637A mutant protein solutions (10 μM)

were titrated with each inhibitor (100 μM in 1% v/v DMSO) by adding 1 μL of injectant to the protein solution at intervals of 4 minutes. The titration of a GST-SH2 domain in PBS solution containing 1% DMSO v/v with the same inhibitor solutions was used as blank test and to determine the heat of dilution of ligand. This reference experiment, carried out in the same way as the titration with protein sample, was subtracted from the sample data. The corrected binding isotherms were fitted to yield the values of the binding constant (K_d), the stoichiometry (n), and the binding enthalpy (ΔH) of each STAT3 SH2 domain/inhibitor binding event. Once the K_d for each inhibitor/protein was determined, the corresponding free energy of binding ΔG_{bind} and the IC_{50} values were obtained via the above mentioned relationship: $\Delta G_{bind} = -RT \ln K_d = -RT \ln 1/IC_{50}$.

2.8. Circular dichroism

CD spectra from GSH-SH2 domain WT, GST-SH2S636A or GST-SH2V637A mutants (0.1 mg ml^{-1} in 10 mM NaPO4, pH 7.4) were recorded on a Chirascan spectropolarimeter (Applied Photophysics) over the wavelength range from 195 to 260 nm at a band width of 1 nm, step size of 0.5 nm and 1s per step. The spectra in the far-ultraviolet region required an average of five scans and were subtracted from blank spectra performed with GST in buffer.

3. RESULTS

3.1. *In silico* analysis of the binding of OPB-31121 to STAT3

We used various computational approaches to examine *in silico* the binding of OPB-31121 (Hayakawa et al., 2013; Kim et al., 2013b) to STAT3 (Fig. 1A). For comparison in our analyses we considered other selected STAT3i, like STA-21 (Song et al., 2005), Stattic (Schust et al., 2006), S3I.201 (Siddiquee et al., 2007) and Cryptotanshinone (Shin et al., 2009), for which there was

some previous evidence of binding to the STAT3 SH2 domain. OPB-31121 was docked onto the SH2 domain and then the relevant drug/protein affinities were scored by molecular dynamics simulation (MDS) (Fig. 1B). The same approach was used for the other compounds (Fig. S1). Tables 1 and S1 show the values of the calculated IC_{50}, free energy of binding ΔG_{bind} and the enthalpic and entropic components predicted for the interaction of each compound with the SH2 domain obtained from the *in silico* analyses. The calculated IC_{50} value for OPB-31121 was in the low nanomolar range (IC_{50},~18 nM). Notably, this value was about 2-3 orders of magnitude lower than the IC_{50} estimated for the other STAT3i, which ranged from 1.4 to 27.2 μM.

To understand the basis of the remarkable high affinity of OPB-31121 for STAT3 we performed a per-residue deconvolution analysis of the free energy of binding (Fig. 1C). The resulting interaction spectrum showed that the residues mostly involved in OPB-31121 binding clustered in two regions. Region 1 included residues from Q635 to E638 and region 2 included residues from T714 to T717. Other four residues (i.e., W623, K626, I659, and V667) were found to be engaged in major stabilizing interactions with OPB-31121. The same procedure was applied to the other STAT3i leading to the definition of the STAT3 interaction spectra for each of these compounds (Fig. S1E-H). Interestingly, the interaction spectra were compound-specific with very little, if any, overlap between them. The interaction region defined for OPB-31121 was clearly distinct from those of the other STAT3i. A visual representation of these results is given in Fig. 1D, where each drug/STAT3 interaction surface is represented in a different color. Thus, our *in silico* data indicated that OPB-31121 bound with remarkably high affinity to the STAT3 SH2 domain and that the binding occurred in a distinct pocket and with different residue specificity compared to other STAT3i.

3.2 *In vitro* assessment of the binding of OPB-31121 to the STAT3 SH2 domain

The binding of OPB-31121 to the SH2 domain of STAT3 was investigated *in vitro* using isothermal titration calorimetry (ITC). Consistent with *in silico* data, ITC demonstrated high affinity binding of OPB-31121 to recombinant GST-tagged STAT3 SH2 domain yielding an experimental K_d of 10 nM (Fig. 2A). For comparison we assessed binding of the other STAT3i using ITC in the same experimental conditions. S3I.201 bound to the SH2 domain with substantially lower affinity compared to OPB-31121 (K_d = 8 μM) (Fig. 2B). All other STAT3i showed similarly low affinity binding with experimental K_d in the micromolar range (Fig. S2). Notably, these data were in good agreement with the estimated IC_{50} values determined by MDS (Table 1). ITC binding experiments were conducted also with GST protein alone to rule out non-specific binding. None of tested compounds showed any interaction with GST (Fig. S3). Hence, the *in vitro* binding assays supported the computational chemistry prediction of high affinity binding of OPB-31121 to the STAT3 SH2 domain.

In addition to higher binding affinity, the *in silico* analyses predicted also substantially distinct binding sites for OPB-31121 and the other STAT3i. In order to test the reliability of this prediction we performed competition binding experiments with OPB-31121 and S3I.201. The recombinant GST-tagged STAT3 SH2 domain was incubated first with a saturating concentration of S3I.201 and then titrated with increasing concentrations of OPB-31121 (Fig. 2C). As predicted by the *in silico* data, OPB-31121 binding was not affected by the pre-incubation with S3I.201 showing similar Kd as in the absence of S3I.201. These data confirmed the presence of independent, non-overlapping binding pockets in the STAT3 SH2 domain for OPB-31121 and other known STAT3i.

3.3 *In silico* alanine scanning and *in vitro* site-directed mutagenesis analysis of the OPB-31121 binding site

To further validate the predicted binding site for OPB-31121 in the STAT3 SH2 domain, we selected two residues (S636 and V637) in the drug-target interaction region defined by binding energy deconvolution analysis. The role of these two residues was first tested *in silico* by alanine scanning mutagenesis (Fig. 3A-B). Turning either the S636 or V637 residue into alanine affected the positioning of OPB-31121 in the binding pocket and greatly reduced the binding affinity resulting in a dramatic increase in the estimated IC_{50} values to 5 μM and 1.1 μM for S636A and V637A, respectively (Table 2). As proof of the specificity, we applied the same approach to S3I.201. Consistent with the predicted difference in the site of interaction, neither the S636A nor V637A mutation affected significantly the binding mode and the estimated binding affinity of S3I.201 (Fig. 3C-D and Table 2).

In parallel with the *in silico* studies, we performed *in vitro* site-directed mutagenesis for the same residues on the GST-tagged STAT3 SH2 domain and assessed binding by ITC. Correct folding of the mutated SH2 domain was determined by comparing circular dichroism (CD) spectra of the wild-type and mutant protein (Fig. S4). Both wild type and mutant SH2 domains displayed the typical SH2 spectra indicating that the mutations did not affect the native conformation of the protein. The S636A and V637A mutations abrogated binding of OPB-31121 in ITC experiments, sustaining the validity of the computational model (Fig. 3E-F). Interestingly, the binding of the reference compound S3I.201 to the STAT3 SH2 domain was not affected by either mutation, showing binding affinities similar to that for the wild-type domain (Fig. 3G-H).

3.4 Inhibition of Y705 and S727 STAT3 phosphorylation by OPB-31121

Next, we assessed the ability of OPB-31121 to interfere with STAT3 phosphorylation at the Y705 and S727 residues in cancer cells. Direct STAT3i would be expected to inhibit the binding of multiple kinases to STAT3 and likely prevent phosphorylation of both Y705 and S727. In these assays, we used two prostate cancer cell lines that exhibited constitutive (DU145) and IL-6 inducible (LNCaP) Y705 phosphorylation, respectively. Cells were treated with increasing concentrations of OPB-31121 for 16 h. IL-6 was added to LNCaP cells during the last 30 min of the incubation to induce pY705. OPB-31121 at concentrations $\geq$ 5 nM strongly inhibited pY705 in both cell lines (Fig. 4A-B). We next determined the kinetics of pY705 inhibition using a dose of 10 nM of OPB-31121. Significant reduction of STAT3 pY705 was achieved within 4-8 h of incubation in both cell lines (Fig.4C-D). We assessed in parallel the effect of OPB-31121 on pS727, which in both DU145 and LNCaP cells is constitutively phosphorylated. Interestingly, OPB-31121 reduced pS727 with dose dependence and kinetics similar to those observed for pY705 inhibition in both cell lines (Fig. 4A-D).

We performed similar experiments with the other STAT3i. All the compounds inhibited pY705 (Fig. 5A). However, even for the most potent of these compounds (cryptotanshinone) doses $\geq$ 5 μM were needed to significantly affect pY705. S3I.201, STA-21 and Stattic were active at doses $\geq$ 20 μM to inhibit pY705 to a comparable level. Notably, these differences in potency reflected closely the differences in the binding affinity between OPB-31121 and the other STAT3i. Interestingly, when we examined the kinetics of inhibition of pY705 and pS727 by cryptotanshinone and S3I.201 a reduction of pY705 was seen within 4 h (Fig. S5A-B). However, significant inhibition of pS727 required longer incubation time (8-16 h). Collectively, these experiments showed that OPB-31121, like other STAT3i, reduced both pY705 and pS727. OPB-31121 acted at low doses and within few hours of incubation on both pY705 and pS727. Furthermore, the activity of OPB-31121 was not

influenced by the preexisting phosphorylation status of STAT3 and similar effects were seen in cells with constitutive and inducible phosphorylation at Y705. Notably, in these cellular assays OPB-31121 was about 100 to 1000 fold more potent than the other STAT3i tested here, in line with the high *in vitro* binding affinity of this compound for STAT3.

3.5 Antiproliferative activity of OPB-31121 in prostate cancer cells

OPB-31121 has been recently reported to have anticancer activity in various preclinical cancer models (Hayakawa et al., 2013; Kim et al., 2013b). However, the drug has never been tested in prostate cancer cells. STAT3 activation and increased Y705 and S727 phosphorylation are frequent in human prostate cancer both at the early (androgen-dependent) and late (castration-resistant) stages of the disease and are generally associated with poor clinical outcome (Culig et al., 2005; Dhir et al., 2002; Mora et al., 2002). Thus, in prostate cancer the availability of compounds that could effectively block pY705 and pS727 and STAT3 signaling through the corresponding downstream pathways could be highly advantageous. Hence, we assessed the effects of OPB-31121 on proliferation of LNCaP and DU145 cells, which are common models of androgen-dependent and castration-resistant prostate cancer, respectively. OPB-31121 inhibited LNCaP and DU145 cell proliferation very effectively with IC_{50} values in nanomolar range (18 and 25 nM) (Fig. 6A). Colony formation was also strongly inhibited by OPB-31121 at doses of 10-50 nM (Fig. 6B). For comparison we tested the effects of the other STAT3i in both cell lines. All the compounds affected cell proliferation, but the doses required to achieve significant effects were significantly higher than those of OPB-31121 (Fig. 6A). Higher doses of these STAT3i were also required in the clonogenic assays (Fig. 6B). Thus, in line with the higher binding affinity, OPB-31121 was substantially more potent in suppressing cell proliferation and colony formation compared to other STAT3i.

4. DISCUSSION

STAT3 is a latent cytoplasmic transcription factor whose activity is controlled by various post-translational modifications (Yu et al., 2014; Yu et al., 2009). Phosphorylation at Y705 enhance nuclear localization and transcriptional activity of STAT3, while pS727 has been reported to control localization and activity of STAT3 in mitochondria (Levy and Darnell, 2002; Yu et al., 2014; Yu et al., 2009). STAT3 has an important role in human cancers sustaining neoplastic transformation and promoting tumor progression (Yu et al., 2009). Therefore, there is high interest in developing STAT3i for cancer therapy (Debnath et al., 2012). OPB-31121 has been recently reported to inhibit STAT3 signaling and has relevant anticancer activity in preclinical models *in vitro* and *in vivo* (Hayakawa et al., 2013; Kim et al., 2013b). Based on its activity in preclinical models clinical trials have been initiated with OPB-31121 and are currently ongoing (Hayakawa et al., 2013; Kim et al., 2013b). Despite its proven efficacy of OPB-31121 in preclinical models, questions remain about its intracellular target and mechanism of action. In this study, we combined computational and experimental approaches to define the mode of interaction of OPB-31121 with STAT3. For comparison, we performed similar studies with a series of structurally distinct STAT3i. To our knowledge, a detailed study of how different small molecules interact with the SH2 domain of STAT3 and how their binding mode impact on the biological activity of the compounds is missing. Indeed, even slight differences in the interaction site and binding affinity might be highly relevant in terms of biological activity and potency of the compounds. Interestingly, we found that OPB-31121 has a remarkably high affinity for STAT3 and unique mode of interaction with the SH2 domain compared to other STAT3i.

We used computational docking and MDS to examine the potential binding site of OPB-31121 in the SH2 domain of STAT3. The residues in the SH2 domain lining the putative site of binding were

identified and those affording the major stabilizing contribution to the binding were investigated by free energy deconvolution and *in silico* alanine scanning mutagenesis. The same computational procedures were applied to the other STAT3i with the purpose of a direct comparison of the binding modes and sites of interaction. Importantly, these computational predictions were validated by *in vitro* binding assays using ITC and recombinant STAT3 SH2 domain. Both series of experiments concurred to show that OPB-31121 binds to STAT3 in the SH2 domain with very low Kd. Indeed, both the computationally and experimentally estimated K_d values for OPB-31121 were 2-3 orders of magnitude lower than those of the other STAT3i tested in this study. Notably, a similar ranking of the compounds was obtained in the cell-based assays based on their efficacy on STAT3 phosphorylation and cell proliferation. All the data confirmed the substantially higher potency of OPB-31121 compared to the other STAT3i.

In greater details, our *in silico* analysis identified two distinct binding pockets for small molecule inhibitors in the SH2 domain of STAT3: the first is occupied by OPB-31121 and the second pocket is common to all other inhibitors tested (Fig.1D). The crystal structure of the STAT3-SH2 domain revealed the existence of one hydrophilic and two hydrophobic sub-pockets (Becker et al., 1998). Most STAT3i are predicted to bind either to the hydrophilic site, lined by the side chains of the K591, R609, S611, and S613 residues, or to a partially hydrophobic region composed by the K592, R595, I597, and I634 residues (Fletcher et al., 2008). Our computational analyses confirmed that all four STAT3i considered here (i.e., cryptotanshinone, STA-21, Stattic, and S3I-201) fit in these two sub-pockets (Fig. 1D and Fig. S1). In contrast, OPB-31121 was found to bind to a distinct region that included the third, hydrophobic sub-pocket (Fig. 1B-C). OPB-31121 interacted also with a consistently larger number of residues in the SH2 domain compared to the other compounds; this in turn contributed to the higher affinity of OPB-31121 for STAT3, as indicated by the extremely favorable comparison of estimated IC_{50} (Table 1) and K_d values (Fig. 2A).

The ITC experiments concurred to support the *in silico* model of the interaction of OPB-31121 and the other STAT3i with the STAT3 SH2 domain. Competition experiments and site-directed mutagenesis showed the specificity of the interaction site of OPB-31121 in the SH2 domain (Fig. 2-3). The presence of a distinct sub-pocket and the high binding affinity of OPB-31121 explain in part the high efficacy of the compound in inhibiting STAT3 phosphorylation in cells. Furthermore, in the case of OPB-31121 inhibition of pY705 and pS727 occurred at similar doses and within the same time scale (~4h) (Fig. 4). This was not the case with other STAT3i, like cryptotanshinone and S3I.201, for which the inhibition of pS727 was delayed with respect to pY705 inhibition (Fig. S5). Thus, occupying a wider and distinct area in the SH2 domain, OPB-31121 could impair more effectively the interaction of STAT3 with kinases and other proteins and prevent simultaneously and with higher efficiency phosphorylation of these critical residues than other STAT3i. Collectively, our results demonstrate that OPB-31121 binds to the SH2 domain and interferes directly with STAT3 activation and signaling. Higher binding affinity is likely to lead to higher potency in cellular assays and *in vivo*, although the compound's propensity to be internalized in cells and metabolized could influence its efficacy in biological systems.

Interfering with JAK/STAT3 signaling has been proposed as a valid option for treatment of prostate cancer (Hedvat et al., 2009; Kroon et al., 2013; Schroeder et al., 2014). However, blocking pY705 alone may not be sufficient. pS727 is frequently increased in human prostate tumors and has been shown to be sufficient to drive prostate tumorigenesis and progression even independently of pY705 (Qin et al., 2008). Furthermore, in preclinical models of prostate cancer inactivation of pS727 is sufficient to substantially reduce tumorigenicity (Qin et al., 2008). In line with the prominent activation of STAT3 signaling in prostate cancer (Culig et al., 2005; Dhir et al., 2002; Mora et al., 2002), we tested the activity of OPB-31121 in two prostate cancer cell lines,

LNCaP and DU145, representative of androgen-dependent and castration-resistant tumors, respectively. We found that OPB-31121 was a potent inhibitor of proliferation and clonogenicity in both cell models (Fig. 6). Interestingly, the antiproliferative effect of OPB-31121 was independent of the pY705 status and apparently related to the ability of the compounds to block effectively and concomitantly both pY705 and pS727. This raises the possibility that the efficacy of OPB-31121 may not depend exclusively on Y705 activation status and that additional factors should be taken in consideration. Together, these findings suggest also that the use of direct STAT3i like OPB-31121 might be expanded to tumors that do not harbor constitutive pY705 and additional biomarkers (e.g., total and pS727 STAT3 protein level) should be considered to identify potentially sensitive tumor types.

ACKNOWLEDGMENTS

We thank Edwin Rock and Dusan Kostic (Otsuka Pharmaceuticals) for their continuous support and helpful comments. This work was supported by a grant from Otsuka Pharmaceuticals, Ticino Foundation for Cancer Research and Foundation Virginia Boeger to C.V.C.

REFERENCES

Becker, S., Groner, B., Muller, C.W., 1998. Three-dimensional structure of the Stat3beta homodimer bound to DNA. Nature 394, 145-151.

Benekli, M., Baumann, H., Wetzler, M., 2009. Targeting signal transducer and activator of transcription signaling pathway in leukemias. J Clin Oncol 27, 4422-4432.

Chan, K.S., Sano, S., Kiguchi, K., Anders, J., Komazawa, N., Takeda, J., DiGiovanni, J., 2004. Disruption of Stat3 reveals a critical role in both the initiation and the promotion stages of epithelial carcinogenesis. J Clin Invest 114, 720-728.

Culig, Z., Steiner, H., Bartsch, G., Hobisch, A., 2005. Interleukin-6 regulation of prostate cancer cell growth. J Cell Biochem 95, 497-505.

Debnath, B., Xu, S., Neamati, N., 2012. Small molecule inhibitors of signal transducer and activator of transcription 3 (Stat3) protein. J Med Chem 55, 6645-6668.

Dhir, R., Ni, Z., Lou, W., DeMiguel, F., Grandis, J.R., Gao, A.C., 2002. Stat3 activation in prostatic carcinomas. Prostate 51, 241-246.

Fletcher, S., Turkson, J., Gunning, P.T., 2008. Molecular approaches towards the inhibition of the signal transducer and activator of transcription 3 (Stat3) protein. ChemMedChem 3, 1159-1168.

Genini, D., Garcia-Escudero, R., Carbone, G.M., Catapano, C.V., 2012. Transcriptional and Non-Transcriptional Functions of PPARbeta/delta in Non-Small Cell Lung Cancer. PLoS One 7, e46009.

Giliberti, G., Ibba, C., Marongiu, E., Loddo, R., Tonelli, M., Boido, V., Laurini, E., Posocco, P., Fermeglia, M., Pricl, S., 2010. Synergistic experimental/computational studies on arylazoenamine derivatives that target the bovine viral diarrhea virus RNA-dependent RNA polymerase. Bioorg Med Chem 18, 6055-6068.

Gough, D.J., Corlett, A., Schlessinger, K., Wegrzyn, J., Larner, A.C., Levy, D.E., 2009. Mitochondrial STAT3 supports Ras-dependent oncogenic transformation. Science 324, 1713-1716.

Grivennikov, S., Karin, M., 2008. Autocrine IL-6 signaling: a key event in tumorigenesis? Cancer Cell 13, 7-9.

Guo, J., Wang, X., Sun, H., Liu, H., Yao, X., 2012. The molecular basis of IGF-II/IGF2R recognition: a combined molecular dynamics simulation, free-energy calculation and computational alanine scanning study. J Mol Model 18, 1421-1430.

Hayakawa, F., Sugimoto, K., Harada, Y., Hashimoto, N., Ohi, N., Kurahashi, S., Naoe, T., 2013. A novel STAT inhibitor, OPB-31121, has a significant antitumor effect on leukemia with STAT-addictive oncokinases. Blood Cancer J 3, e166.

Hedvat, M., Huszar, D., Herrmann, A., Gozgit, J.M., Schroeder, A., Sheehy, A., Buettner, R., Proia, D., Kowolik, C.M., Xin, H., Armstrong, B., Bebernitz, G., Weng, S., Wang, L., Ye, M., McEachern, K., Chen, H., Morosini, D., Bell, K., Alimzhanov, M., Ioannidis, S., McCoon, P., Cao, Z.A., Yu, H., Jove, R., Zinda, M., 2009. The JAK2 inhibitor AZD1480 potently blocks Stat3 signaling and oncogenesis in solid tumors. Cancer Cell 16, 487-497.

Kim, E., Kim, M., Woo, D.H., Shin, Y., Shin, J., Chang, N., Oh, Y.T., Kim, H., Rheey, J., Nakano, I., Lee, C., Joo, K.M., Rich, J.N., Nam, D.H., Lee, J., 2013a. Phosphorylation of EZH2 activates STAT3 signaling via STAT3 methylation and promotes tumorigenicity of glioblastoma stem-like cells. Cancer Cell 23, 839-852.

Kim, M.J., Nam, H.J., Kim, H.P., Han, S.W., Im, S.A., Kim, T.Y., Oh, D.Y., Bang, Y.J., 2013b. OPB-31121, a novel small molecular inhibitor, disrupts the JAK2/STAT3 pathway and exhibits an antitumor activity in gastric cancer cells. Cancer Lett 335, 145-152.

Kortylewski, M., Kujawski, M., Wang, T., Wei, S., Zhang, S., Pilon-Thomas, S., Niu, G., Kay, H., Mule, J., Kerr, W.G., Jove, R., Pardoll, D., Yu, H., 2005. Inhibiting Stat3 signaling in the hematopoietic system elicits multicomponent antitumor immunity. Nat Med 11, 1314-1321.

Kroon, P., Berry, P.A., Stower, M.J., Rodrigues, G., Mann, V.M., Simms, M., Bhasin, D., Chettiar, S., Li, C., Li, P.K., Maitland, N.J., Collins, A.T., 2013. JAK-STAT blockade inhibits tumor initiation and clonogenic recovery of prostate cancer stem-like cells. Cancer Res 73, 5288-5298.

Laurini, E., Col, V.D., Mamolo, M.G., Zampieri, D., Posocco, P., Fermeglia, M., Vio, L., Pricl, S., 2011. Homology Model and Docking-Based Virtual Screening for Ligands of the sigma1 Receptor. ACS Med Chem Lett 2, 834-839.

Laurini, E., Marson, D., Dal Col, V., Fermeglia, M., Mamolo, M.G., Zampieri, D., Vio, L., Pricl, S., 2012. Another brick in the wall. Validation of the sigma1 receptor 3D model by computer-assisted design, synthesis, and activity of new sigma1 ligands. Mol Pharm 9, 3107-3126.

Lee, H., Zhang, P., Herrmann, A., Yang, C., Xin, H., Wang, Z., Hoon, D.S., Forman, S.J., Jove, R., Riggs, A.D., Yu, H., 2012. Acetylated STAT3 is crucial for methylation of tumor-suppressor gene promoters and inhibition by resveratrol results in demethylation. Proc Natl Acad Sci U S A 109, 7765-7769.

Lee, H.J., Zhuang, G., Cao, Y., Du, P., Kim, H.J., Settleman, J., 2014. Drug resistance via feedback activation of Stat3 in oncogene-addicted cancer cells. Cancer Cell 26, 207-221.

Levy, D.E., Darnell, J.E., Jr., 2002. Stats: transcriptional control and biological impact. Nat Rev Mol Cell Biol 3, 651-662.

Lim, C.P., Cao, X., 2006. Structure, function, and regulation of STAT proteins. Mol Biosyst 2, 536-550.

Marotta, L.L., Almendro, V., Marusyk, A., Shipitsin, M., Schemme, J., Walker, S.R., Bloushtain-Qimron, N., Kim, J.J., Choudhury, S.A., Maruyama, R., Wu, Z., Gonen, M., Mulvey, L.A., Bessarabova, M.O., Huh, S.J., Silver, S.J., Kim, S.Y., Park, S.Y., Lee, H.E., Anderson, K.S., Richardson, A.L., Nikolskaya, T., Nikolsky, Y., Liu, X.S., Root, D.E., Hahn, W.C., Frank, D.A., Polyak, K., 2011. The JAK2/STAT3 signaling pathway is required for growth of CD44(+)CD24(-) stem cell-like breast cancer cells in human tumors. J Clin Invest 121, 2723-2735.

Meier, J.A., Larner, A.C., 2014. Toward a new STATe: the role of STATs in mitochondrial function. Semin Immunol 26, 20-28.

Mora, L.B., Buettner, R., Seigne, J., Diaz, J., Ahmad, N., Garcia, R., Bowman, T., Falcone, R., Fairclough, R., Cantor, A., Muro-Cacho, C., Livingston, S., Karras, J., Pow-Sang, J., Jove, R.,

2002. Constitutive activation of Stat3 in human prostate tumors and cell lines: direct inhibition of Stat3 signaling induces apoptosis of prostate cancer cells. Cancer Res 62, 6659-6666.

Morris, G.M., Huey, R., Lindstrom, W., Sanner, M.F., Belew, R.K., Goodsell, D.S., Olson, A.J., 2009. AutoDock4 and AutoDockTools4: Automated docking with selective receptor flexibility. J Comput Chem 30, 2785-2791.

Napoli, S., Pastori, C., Magistri, M., Carbone, G.M., Catapano, C.V., 2009. Promoter-specific transcriptional interference and c-myc gene silencing by siRNAs in human cells. EMBO J 28, 1708-1719.

O'Shea, J.J., Plenge, R., 2012. JAK and STAT signaling molecules in immunoregulation and immune-mediated disease. Immunity 36, 542-550.

Qin, H.R., Kim, H.J., Kim, J.Y., Hurt, E.M., Klarmann, G.J., Kawasaki, B.T., Duhagon Serrat, M.A., Farrar, W.L., 2008. Activation of signal transducer and activator of transcription 3 through a phosphomimetic serine 727 promotes prostate tumorigenesis independent of tyrosine 705 phosphorylation. Cancer Res 68, 7736-7741.

Sansone, P., Bromberg, J., 2012. Targeting the interleukin-6/Jak/stat pathway in human malignancies. J Clin Oncol 30, 1005-1014.

Schroeder, A., Herrmann, A., Cherryholmes, G., Kowolik, C., Buettner, R., Pal, S., Yu, H., Muller-Newen, G., Jove, R., 2014. Loss of androgen receptor expression promotes a stem-like cell phenotype in prostate cancer through STAT3 signaling. Cancer Res 74, 1227-1237.

Schust, J., Sperl, B., Hollis, A., Mayer, T.U., Berg, T., 2006. Stattic: a small-molecule inhibitor of STAT3 activation and dimerization. Chem Biol 13, 1235-1242.

Shin, D.S., Kim, H.N., Shin, K.D., Yoon, Y.J., Kim, S.J., Han, D.C., Kwon, B.M., 2009. Cryptotanshinone inhibits constitutive signal transducer and activator of transcription 3 function through blocking the dimerization in DU145 prostate cancer cells. Cancer Res 69, 193-202.

Siddiquee, K., Zhang, S., Guida, W.C., Blaskovich, M.A., Greedy, B., Lawrence, H.R., Yip, M.L., Jove, R., McLaughlin, M.M., Lawrence, N.J., Sebti, S.M., Turkson, J., 2007. Selective chemical probe inhibitor of Stat3, identified through structure-based virtual screening, induces antitumor activity. Proc Natl Acad Sci U S A 104, 7391-7396.

Song, H., Wang, R., Wang, S., Lin, J., 2005. A low-molecular-weight compound discovered through virtual database screening inhibits Stat3 function in breast cancer cells. Proc Natl Acad Sci U S A 102, 4700-4705.

Sos, M.L., Levin, R.S., Gordan, J.D., Oses-Prieto, J.A., Webber, J.T., Salt, M., Hann, B., Burlingame, A.L., McCormick, F., Bandyopadhyay, S., Shokat, K.M., 2014. Oncogene mimicry as a mechanism of primary resistance to BRAF inhibitors. Cell Rep 8, 1037-1048.

Su, Y.J., Lai, H.M., Chang, Y.W., Chen, G.Y., Lee, J.L., 2011. Direct reprogramming of stem cell properties in colon cancer cells by CD44. EMBO J 30, 3186-3199.

Timofeeva, O.A., Chasovskikh, S., Lonskaya, I., Tarasova, N.I., Khavrutskii, L., Tarasov, S.G., Zhang, X., Korostyshevskiy, V.R., Cheema, A., Zhang, L., Dakshanamurthy, S., Brown, M.L., Dritschilo, A., 2012. Mechanisms of unphosphorylated STAT3 transcription factor binding to DNA. J Biol Chem 287, 14192-14200.

Toso, A., Revandkar, A., Di Mitri, D., Guccini, I., Proietti, M., Sarti, M., Pinton, S., Zhang, J., Kalathur, M., Civenni, G., Jarrossay, D., Montani, E., Marini, C., Garcia-Escudero, R., Scanziani, E., Grassi, F., Pandolfi, P.P., Catapano, C.V., Alimonti, A., 2014. Enhancing Chemotherapy Efficacy in Pten-Deficient Prostate Tumors by Activating the Senescence-Associated Antitumor Immunity. Cell Rep.

Wegrzyn, J., Potla, R., Chwae, Y.J., Sepuri, N.B., Zhang, Q., Koeck, T., Derecka, M., Szczepanek, K., Szelag, M., Gornicka, A., Moh, A., Moghaddas, S., Chen, Q., Bobbili, S., Cichy, J., Dulak, J., Baker, D.P., Wolfman, A., Stuehr, D., Hassan, M.O., Fu, X.Y., Avadhani, N., Drake, J.I., Fawcett,

P., Lesnefsky, E.J., Larner, A.C., 2009. Function of mitochondrial Stat3 in cellular respiration. Science 323, 793-797.

Wen, Z., Zhong, Z., Darnell, J.E., Jr., 1995. Maximal activation of transcription by Stat1 and Stat3 requires both tyrosine and serine phosphorylation. Cell 82, 241-250.

Yu, H., Lee, H., Herrmann, A., Buettner, R., Jove, R., 2014. Revisiting STAT3 signalling in cancer: new and unexpected biological functions. Nat Rev Cancer 14, 736-746.

Yu, H., Pardoll, D., Jove, R., 2009. STATs in cancer inflammation and immunity: a leading role for STAT3. Nat Rev Cancer 9, 798-809.

Yuan, Z.L., Guan, Y.J., Chatterjee, D., Chin, Y.E., 2005. Stat3 dimerization regulated by reversible acetylation of a single lysine residue. Science 307, 269-273.

Zhang, X., Blenis, J., Li, H.C., Schindler, C., Chen-Kiang, S., 1995. Requirement of serine phosphorylation for formation of STAT-promoter complexes. Science 267, 1990-1994.

Zhong, Z., Wen, Z., Darnell, J.E., Jr., 1994. Stat3: a STAT family member activated by tyrosine phosphorylation in response to epidermal growth factor and interleukin-6. Science 264, 95-98.

Table 1. Predicted free energy of binding (ΔG_{bind}) and IC_{50} values for OPB-31121, Cryptotanshinone, STA-21, S3I.201, and Stattic in complex with STAT3.

	OPB-31121	STA-21	Stattic	Crypto	S3I.201
ΔG_{bind} (kcal/mol)	-10.54 ± 0.77	-6.47 ± 0.88	-6.99 ± 0.79	-8.01 ± 0.61	-6.23 ± 0.89
IC_{50} (μM)[a]	0.0187	17.900	7.400	1.400	27.200

[a] ΔG_{bind} and IC_{50} of ligand are related by the following fundamental equation: $\Delta G_{bind} = -RT \ln 1/IC_{50}$, where R is the gas constant and T is the temperature. Once ΔG_{bind} for a given protein/ligand couple is estimated by MM-PBSA simulations, the relative IC_{50} value is determined by virtue of this relationship.

Table 2. Predicted free energy of binding (ΔG_{bind}), binding energy difference ($\Delta\Delta G_{bind}$ = ΔG_{bind}(wild type) – ΔG_{bind}(mutant), and IC_{50} values for OPB-31121 and S3I.201 with S636A and V637A STAT3 mutants.

	S636A		V637A	
	OPB-31121	S3I.201	OPB-31121	S3I.201
ΔG_{bind} (kcal/mol)	-7.23 ± 0.64	-6.15 ± 0.67	-8.11 ± 0.69	-6.26 ± 0.78
$\Delta\Delta G_{bind}$ (kcal/mol)	-3.31	-0.08	-2.43	+0.03
IC_{50} (μM)	5	31.2	1.1	25.9

FIGURE LEGENDS

Figure 1. *In silico* binding of OPB-31121 to STAT3. (*A*) Three-dimensional structure of the STAT3 protein. The different domains of STAT3 are indicated in different colors indicated both in the structure and diagram. (*B*) Details of the binding site of OPB-31121 in the STAT3 SH2 domain obtained from equilibrated MDS snapshots. The protein backbone is portrayed as a transparent sky blue ribbon; the main residues involved in drug interactions are shown as labeled colored sticks. OPB-31121 is portrayed as atom-colored sticks-and-balls. (*C*) Interaction spectrum for STAT3 in complex with OPB-31121. Only residues for which ΔG_{bind} is $\geq$ 0.75 kcal/mol are shown. (*D*) Binding pockets of different inhibitors on the STAT3 SH2 domain highlighted by their respective van der Waals surfaces. Dark gray, SH2 domain; blue, OPB-31121; yellow, STA-21; red, cryptotanshinone; green, S3I.201. Stattic is hidden by cryptotanshinone that binds to an overlapping site.

Figure 2. *In vitro* binding of OPB-31221 to the STAT3 SH2 domain. (*A*) Isothermal titration calorimetry (ITC) data for the STAT3 SH2 domain/OPB-31121 system. (*B*) ITC data for the STAT3 SH2 domain/S3I.201 system. (*C*) ITC analysis of OPB-31121 interaction with the STAT3 SH2 domain after pre-incubation with S3I.201.

Figure 3. Mutational analysis of OPB-31121 binding site in the STAT3 SH2 domain. (*A*) Superposition of the binding site of wild type (light blue) and S636A STAT3 mutant (orange) in complex with OPB-31221. (*B*) Superposition of the binding site of wild type (light blue) and V637A STAT3 mutant (golden rod) in complex with OPB-31221. (*C*) Superposition of the binding site of wild type (aquamarine) and S636A STAT3 mutant (sandy brown) in complex with S3I.201.

(*D*) Superposition of the binding site of wild type (aquamarine) and V637A STAT3 mutant (salmon) in complex with S3I.201. In all panels drugs are depicted as colored sticks-and-balls, while main residues involved in the interactions are labeled and shown as colored sticks. Hydrogen atoms, water molecules, ions and counterions are omitted for clarity. (*E*) ITC data for S636A mutant STAT3 SH2 domain in complex with OPB-31121. (*F*) ITC data for V637A mutant STAT3 SH2 domain in complex with OPB-31121; (G) ITC data for S636A mutant STAT3 SH2 domain in complex with S3I.201; (*H*) ITC data for V637A mutant STAT3 SH2 domain in complex with S3I.201.

Figure 4. Inhibition of STAT3 phosphorylation at Y705 and S727 by OPB-31121. (*A*-*B*) STAT3 phosphorylation in DU145 (*A*) and LNCaP (*B*) cells treated with the indicated concentrations of OPB-31121 for 16 h. (*C*-*D*) STAT3 phosphorylation in DU145 (*C*) and LNCaP *(D*) cells incubated with OPB-31121 (10 nM) and analyzed at the indicated times. IL-6 was added for 30 min at the end of the treatment with OPB-31121 to induce pY705.

Figure 5. Inhibition of STAT3 phosphorylation at Y705 by STA-21, Stattic, Cryptotanshinone, and S3I.201 for 16 h in DU145 (*A*) and LNCaP (*B*) cells.

Figure 6. Inhibition of cell proliferation and colony formation by STAT3 inhibitors. (*A*) Cell viability determined by MTT assay in DU145 and LNCaP cells incubated with the indicated compounds. Left, IC_{50} values for each compound in the two cell lines. (*B*) Anchorage-dependent clonal growth of DU145 and LNCaP cells treated with the indicated doses of OPB31121, STA-21, Stattic, cryptotanshinone, and S3I.201. *$P < 0.01$.

Figure 1

Figure 1

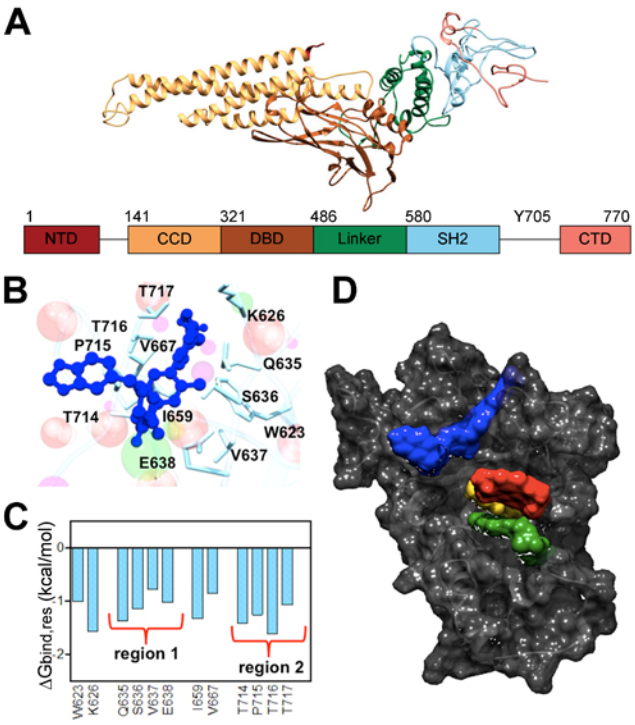

Figure 2

Figure 2

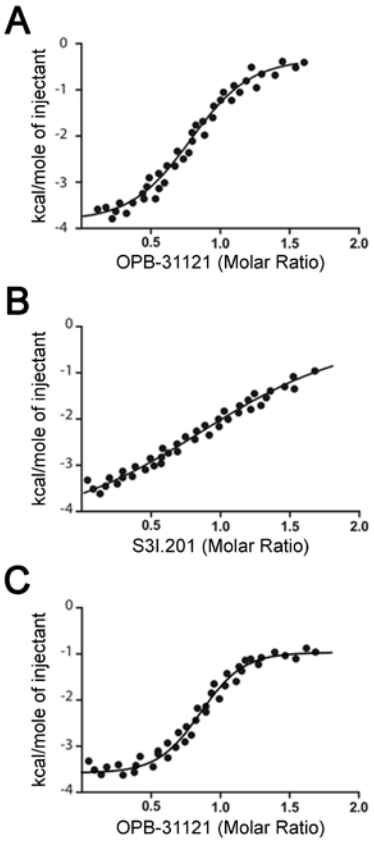

Figure 3

Figure 3

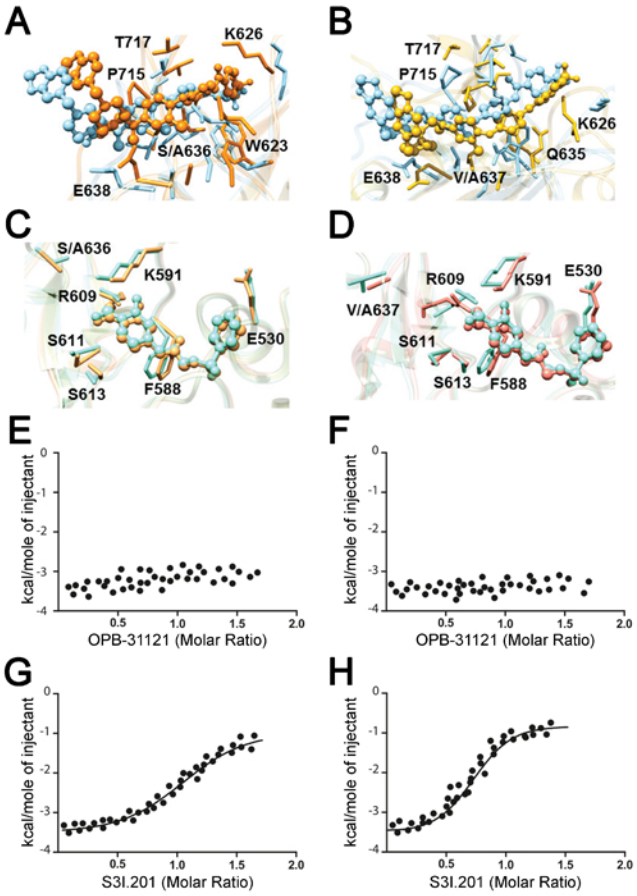

Figure 4

Figure 4

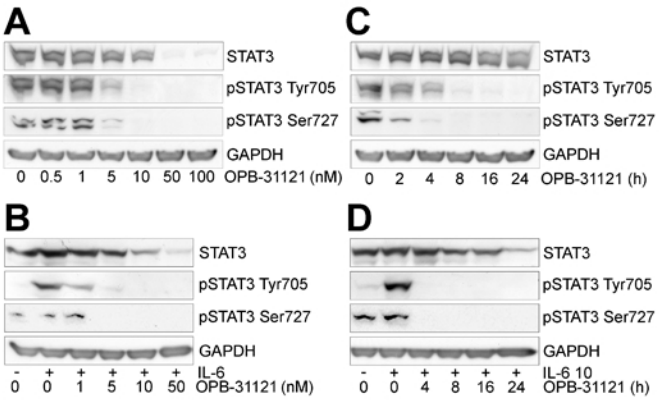

Figure 5

Figure 5

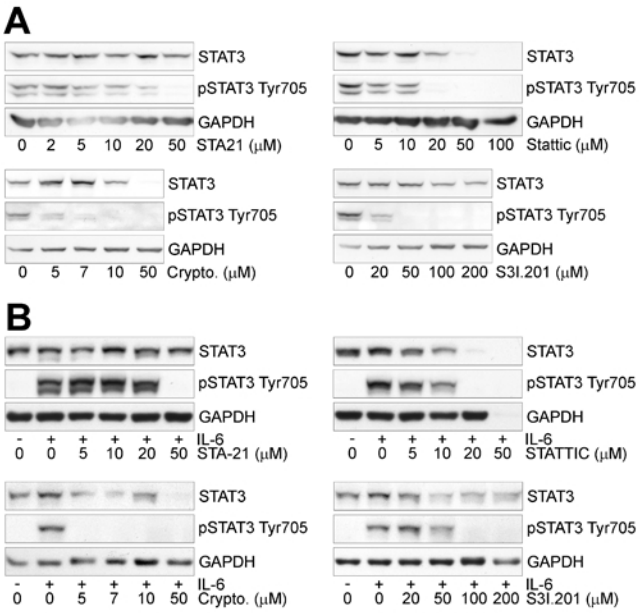

Figure 6

Figure 6

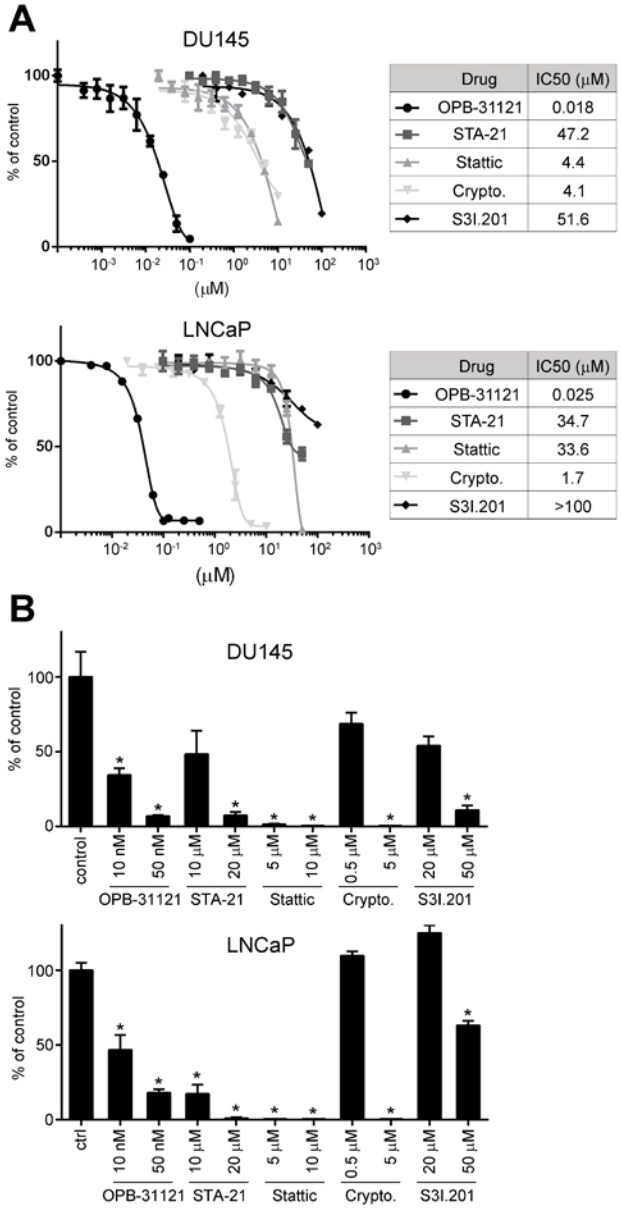

***Highlights**

- STAT3 is an attractive target for development of novel anticancer drugs
- OPB-31121 is a putatively STAT3 inhibitor currently in clinical trials
- OPB-31121 binds with high affinity to the SH2 domain of STAT3
- OPB-31121 binds at a novel site in the SH2 domain distinct from other inhibitors

Figure S1

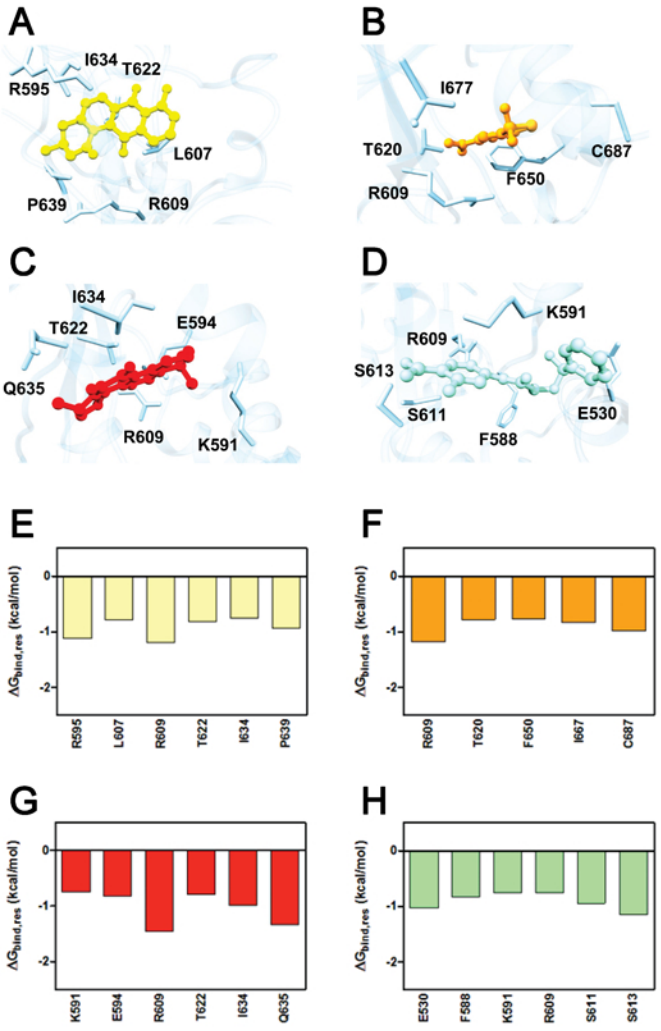
A
I634
T622
R595
L607
P639
R609
B
I677
T620
C687
F650
R609
C
I634
T622
E594
Q635
R609
K591
D
K591
R609
S613
S611
E530
F588
E
ΔGbind,res (kcal/mol)
0
-1
-2
R595
L607
R609
T622
I634
P639
F
ΔGbind,res (kcal/mol)
0
-1
-2
R609
T620
F650
I667
C687
G
ΔGbind,res (kcal/mol)
0
-1
-2
K591
E594
R609
T622
I634
Q635
H
ΔGbind,res (kcal/mol)
0
-1
-2
E530
F588
K591
R609
S611
S613

Figure S2

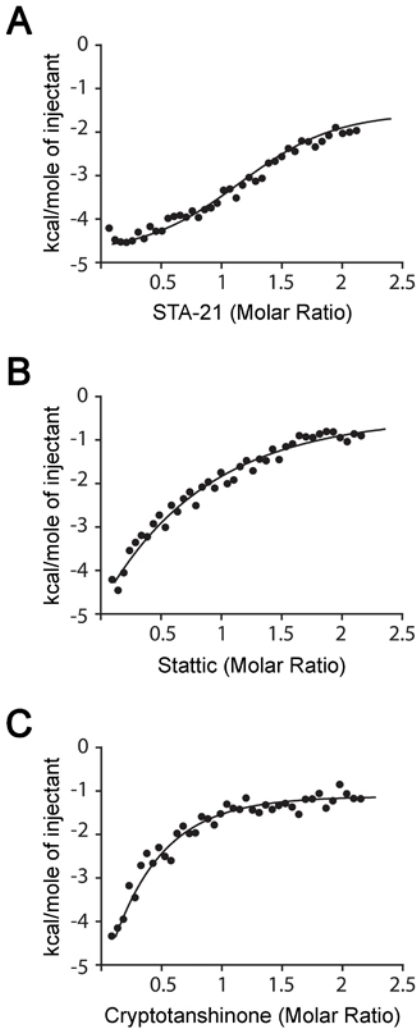
A
kcal/mole of injectant
0
-1
-2
-3
-4
-5
0.5
1
1.5
2
2.5
STA-21 (Molar Ratio)
B
kcal/mole of injectant
Stattic (Molar Ratio)
C
kcal/mole of injectant
Cryptotanshinone (Molar Ratio)

Figure S3

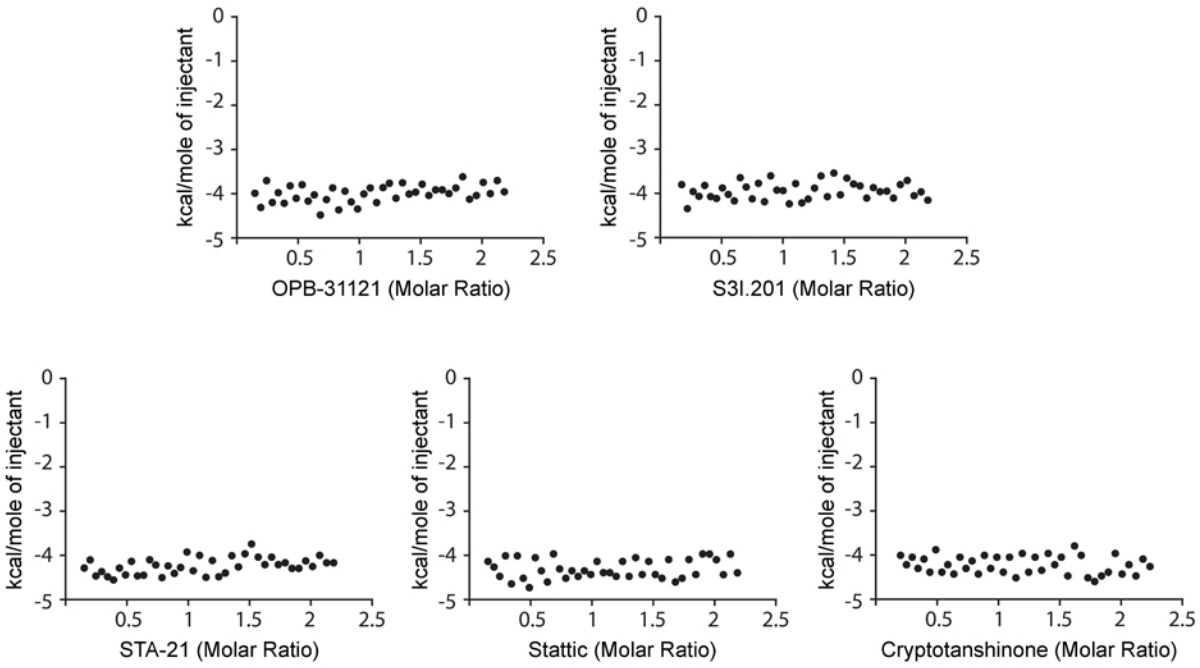
kcal/mole of injectant
0
-1
-2
-3
-4
-5
0.5
1
1.5
2
2.5
OPB-31121 (Molar Ratio)
S3I.201 (Molar Ratio)
STA-21 (Molar Ratio)
Stattic (Molar Ratio)
Cryptotanshinone (Molar Ratio)

Figure S4

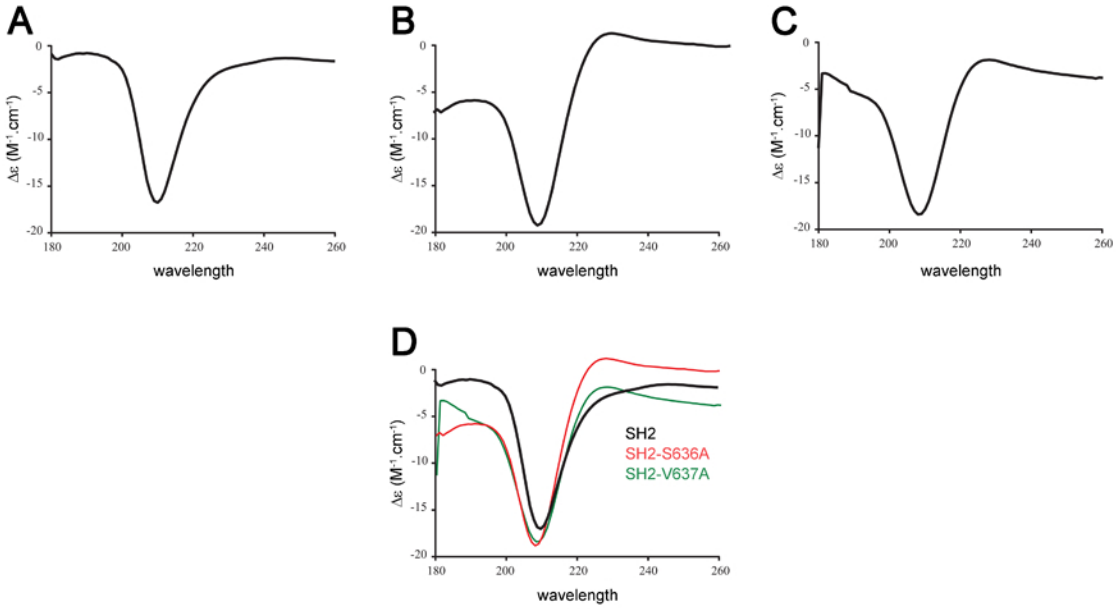

Figure S5

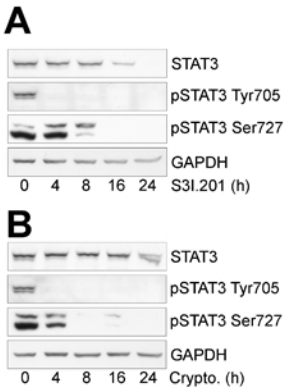
A
STAT3
pSTAT3 Tyr705
pSTAT3 Ser727
GAPDH
0 4 8 16 24 S3I.201 (h)
B
STAT3
pSTAT3 Tyr705
pSTAT3 Ser727
GAPDH
0 4 8 16 24 Crypto. (h)

Supporting Information

This file contains:

a. Supplementary Table S1

b. Supplementary Figure Legends S1-S4

Table S1. Enthalpic (ΔH_{bind}) and entropic ($-T\Delta S_{bind}$) components of the free energy of binding (ΔG_{bind}) predicted for OPB-31121, STA-21, Stattic, Cryptotanshinone and S3I.201 in complex with STAT3.

	OPB-31121	STA-21	Stattic	Cryptotanshinone	S3I.201
ΔH_{bind}, kcal/mol	-27.07 ± 0.65	-18.80 ± 0.66	-17.11 ± 0.66	-8.01 ± 0.49	-19.30 ± 0.69
$-T\Delta S_{bind}$, kcal/mol	16.53 ± 0.42	12.33 ± 0.58	10.12 ± 0.44	14.98 ± 0.36	13.07 ± 0.56
ΔG_{bind}, kcal/mol	-10.54 ± 0.77	-6.47 ± 0.88	-6.99 ± 0.79	-8.01 ± 0.61	-6.23 ± 0.89

Supplementary Figure Legends

Figure S1. *In silico* binding of small molecule inhibitors to STAT3 SH2 domain**.** (A-D) Models of STA-21 (A), Stattic (B), Cryptotanshinone (C), and S3I.201 (D) bound to the SH2 domain of STAT3 as obtained from equilibrated MD simulation snapshots. Inhibitors are portrayed as atom-colored balls-and-sticks. Main residues of the protein involved in the interaction with the drugs are shown as colored sticks and labeled. Hydrogen atoms, water molecules, ions and counterions are omitted for clarity. (E-H) Interaction spectra of STA-21 (*E*), Stattic (*F*), Cryptotanshinone (*G*), and S3I.201 (*H*) with the SH2 domain of STAT3 as obtained from the per-residue deconvolution of the corresponding binding free energy.

Figure S2. Isothermal titration calorimetry (ITC) data for the STAT3 SH2 domain with STA-21 (A), Stattic (B) and Cryptotanshinone (*C*).

Figure S3. Isothermal titration calorimetry (ITC) data for the GST protein/OPB-31121 (A) and GST protein/S3I.201 (B) systems.

Figure S4. Circular dichroism spectra for wild type (*A*), S636A (B) and V637A mutant (C) STAT3 proteins.

Figure S5. Inhibition of STAT3 phosphorylation at Y705 and S727 by cryptotanshinone (7 μM) and S3I.201 (50 μM) in DU-145 cells incubated for the indicated time.